INVESTIGATION OF THE DYNAMIC RESPONSE OF THE EVRIPOS CABLE-STAYED BRIDGE IN GREECE, UNDER ASYNCHRONOUS GROUND MOTION RECORDS

Christos Karakostas[1*], Anastasios Sextos[2], Vassilios Lekidis[1] and Savvas Papadopoulos[2]

[1]Institute of Engineering Seismology & Earthquake Engineering (ITSAK)
5 Agiou Georgou Str., Patriarchika Pylaias, GR55535 Thessaloniki, Greece
christos@itsak.gr , lekidis@itsak.gr

[2]Department of Civil Engineering
Aristotle University of Thessaloniki, Greece
asextos@civil.auth.gr, savvaspp@civil.auth.gr

Keywords: Spatial variation, Cable-stayed bridge, Coherency, Higher modes excitation.

Abstract.

The Evripos bridge in central Greece, connects the island of Evia to the mainland. The cable-stayed section of the bridge is 395m in length, with a central span of 215m and side-spans of 90m each. The deck, 13.5m in width, is at 40m above sea-level, suspended by cables from two, 90m high pylons. A permanent accelerometer special array of 43 sensors was installed on the bridge in 1994 by the Institute of Engineering Seismology and Earthquake Engineering Two triaxial sensors have been monitoring the free-field (near pier M4) and pier M5 base response on the mainland (Boeotean) coast and two others the respective locations (pier base M6 and free-field near pier M7) on the Euboean coast. Since then the bridge's behaviour to seismic excitations has been continuously monitored and investigated. From various earthquake events recorded at the site, it became obvious that the excitation at each of the aforementioned locations differs, with the lowest peak acceleration values observed at site M7 for all three components, independently of magnitude, azimuth and epicentral distance of the earthquake, a fact that can be attributed to local site conditions. In the present research effort, an investigation of the dynamic response of the Evripos bridge due to the asynchronous base excitations along its supports is carried out. Comparisons are made with the conventional design procedure of assuming a common (synchronous) base excitation at all the supports and interesting conclusions are drawn regarding the impact of spatially variable ground motion on the seismic response of the particular bridge.

1 INTRODUCTION

During the last decade, time history analyses have become increasingly popular both for design and research purposes, especially for the case of complex and/or important bridges. This trend has significantly improved the analysis rigor and facilitated the consideration of various physical phenomena that were too complicated to be taken into account in the past. One of those issues, is the identification of a realistic, spatially variable earthquake ground

motion (SVEGM) which can be used for the excitation of the bridge for design or assessment purposes. As it is well known, this phenomenon may affect the seismic response of long bridges, or of bridges crossing abruptly changing soil profiles; however, its potentiallly beneficial or detrimental impact on the final bridge performance cannot be easily assessed in advance ([1]-[5] among others).

One major difficulty in assessing the spatially variable patterns of earthquake ground motion is the complex wave reflections, refractions and superpositions that take place as seismic waves travel within inhomogeneous soil media. Different analytical formulations have been proposed in the past, but the inherent multi-parametric nature of wave propagation and soil-structure interaction makes it practically impossible to predict the spatially varying earthquake input along the bridge length in a deterministic manner. Dense seismograph arrays, primarily in Taiwan, Japan and the U.S., have contributed in shedding some light into this problem which can be primarily attributed to four major factors that take place simultaneously, i.e., wave passage effect, the extended source effect, wave scattering and attenuation effect [6]. The operation of these arrays, also led to the development of numerous empirical, semi-empirical and analytical coherency models, fit to represent the decaying signal correlation with distance and frequency.

Despite the significant impact of the aforementioned analytical approaches and experimental evidence, a reliable and simple methodology for the prediction of the effects of asynchronous motion on bridges is still lacking. Even modern seismic codes like Eurocode 8 deal with the problem through either simplified code-based calculations or indirect measures involving larger seating deck lengths [7].

An interesting case for the study of this phenomenon using recorded data is the Evripos cable-stayed bridge, which has been permanently monitored by an accelerometer network since 1994 [8], [9]. A series of minor to moderate intensity seismic events have been recorded by this network, providing a useful set of motions recorded both in the vicinity of the structure and on specific locations on the structure and its foundation. Scope of this study therefore, is to:

(a) Make use of the recorded data in order to investigate the nature of earthquake ground motion and the effects of its spatial variation on the dynamic response (in terms of forces and displacements) of the particular cable-stayed bridge.

(b) Attempt to correlate the beneficial or detrimental effect of asynchronous motion with the excitation of higher structural modes observed under multiple-support earthquake input.

The description of the bridge, its monitoring system as well as its response under various asynchronous ground motion records, is presented in the following.

2 DESCRIPTION OF EVRIPOS CABLE-STAYED BRIDGE

The Evripos bridge, a 694.5m R/C structure, connects the Euboean coast in the island of Evia to the Boeotean coast in continental central Greece (Figure 1). It is composed of three parts, the central cable stayed section and two side (approaching) parts made of pre-stressed R/C beams that rest on elastomeric bearings. The central section of the bridge is divided into three spans of length 90m, 215m and 90m respectively, while the deck (of 13.50m width) is suspended by the 90m height pylons M5 and M6 with cables. The displacements of the deck along the longitudinal direction are permitted in piers M4 and M7 while those in the trans-

verse direction are blocked [8], [9]. In the present study, it is only the central cable-stayed section that is examined.

As already mentioned, the Evripos cable-stayed bridge behavior is constantly monitored through a special accelerometer array installed by the Institute of Engineering Seismology and Earthquake Engineering (ITSAK). The network is composed by four triaxial accelerometers installed at the base of the bridge, in particular, on the pile caps of piers M5 and M6 and on soil surface in areas adjacent to piers M4 and M7. There are also 31 additional uniaxial accelerometers installed on the superstructure, for system identification purposes. It is noted that all sensors have common time and common trigger settings [8],[9] thus permitting signal processing and correlation. The Finite Element model of the bridge is illustrated in Figure 2.
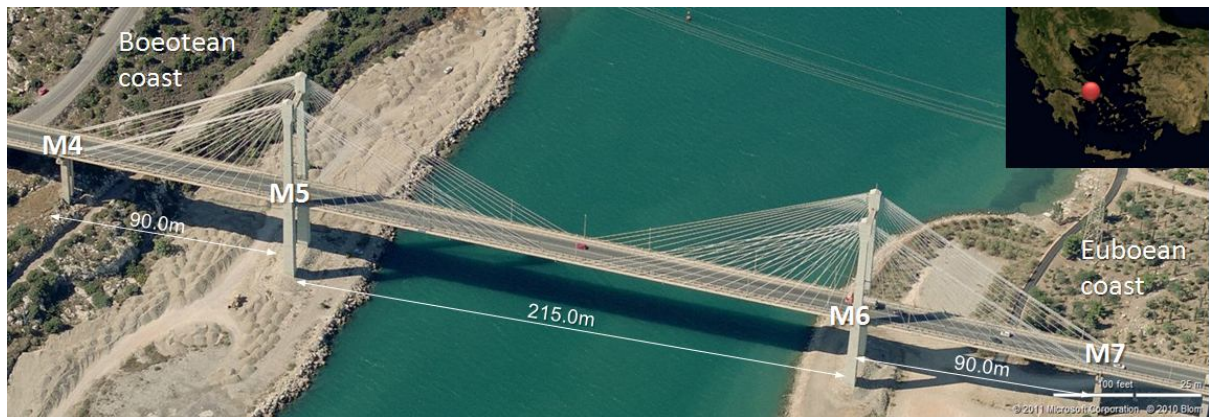

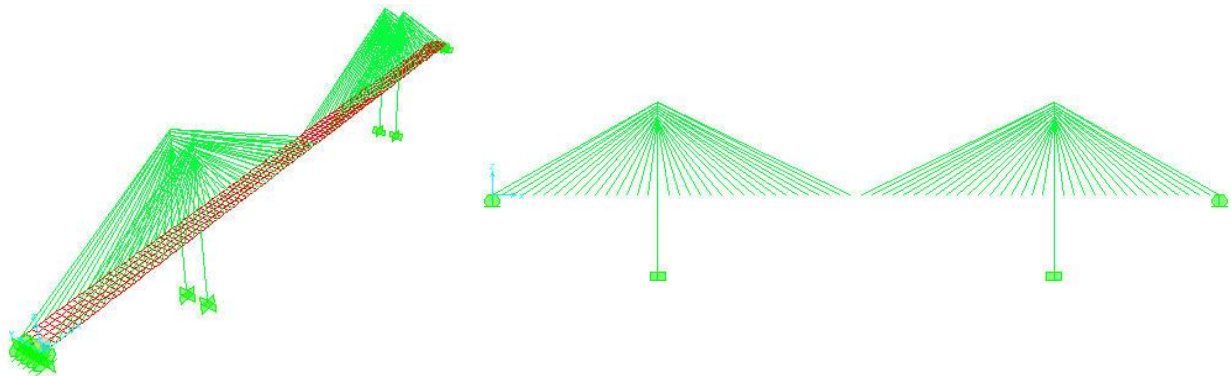Figure 1: The central section of the Evripos cable-stayed bridge.

Figure 2: Finite model of the Evripos cable-stayed bridge.

3 EARTHQUAKE STRONG MOTION DATA AVAILABLE ON SITE

Due to the significant overall length of the central section of the bridge that is almost 400m in total, an effort is made to process specific groups of records available on-site in order to investigate the impact of spatial variability of seismic ground motion. For this purpose, a set of four ground motions was used, as recorded during the Athens earthquake, that occurred on 7/9/1999 at a source-to-site distance of approximately 50km with a surface Magnitude M_s=5.9. The recorded time histories are presented in Figure 3 where the longitudinal, transverse and vertical component is illustrated in different rows for each location. Having ensured that the common time and common trigger condition was fulfilled, the records were first filtered in the frequency range 0.65-25Hz in order to remove the influence of the vibration of the superstruc-

ture which was transmitting waves back to the soil due to inertial soil-structure interaction. Then, the coherency between all pairs of records was computed using a GUI-based, Matlab script written for this purpose. For each individual record, the power spectrum was computed after appropriate smoothing using an 11-point Hamming window as proposed by Abrahamson for 5% structural damping [10], [11]:

$$\bar{S}_{jj}(\omega_n) = \sum_{m=-M}^{+M} W(m\Delta\omega)\hat{S}_{jj}(\omega_n + m\Delta\omega) \qquad (1)$$

where ω_n is the discrete frequency, $W(m\Delta\omega)$ the (Hamming) spectral window and $\hat{S}_{jj}$ the unsmoothed power spectra.
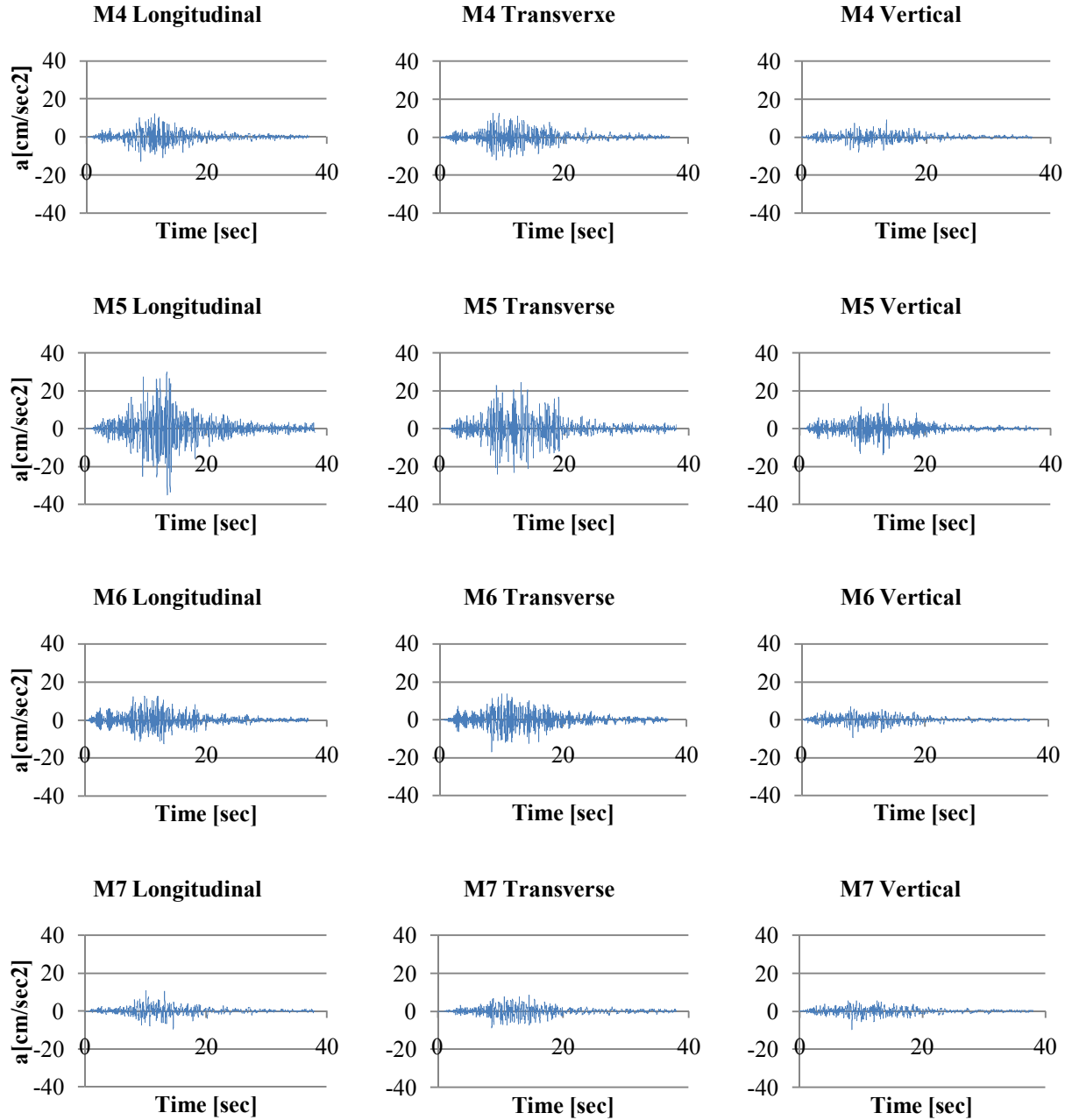
Figure 3: Horizontal and Vertical components of the strong ground motions recorded at the base of piers M4, M5, M6 and M7 due to the 1999 M_s=5.9 Athens earthquake.

Similarly, the smoothed cross spectral densities were calculated for all six pairs of records M_{jk} (i.e., M4-M5, M4-M6, M4-M7, M5-M6, M5-M7, M6-M7) according to the following expression:

$$\bar{S}_{jk}(\omega_n) = \frac{2\pi}{T}\sum_{m=-M}^{+M} W(m\Delta\omega)\Lambda_j(\omega_n + m\Delta\omega)\Lambda_k(\omega_n + m\Delta\omega)\exp\{i[\Phi_\kappa(\omega_n + m\Delta\omega) - \Phi_j(\omega_n + m\Delta\omega)]\} \quad (2)$$

where Λ_j and Λ_k is the Fourier amplitude in stations j and k respectively and Φ_j, Φ_k is the corresponding phase. The lagged coherency, expressing the correlation of the records among all stations, can then be calculated as:

$$\left|\bar{\gamma}_{jk}^M(\omega)\right| = \frac{\left|\bar{S}_{jk}^M(\omega)\right|}{\sqrt{\bar{S}_{jj}^M(\omega)\cdot\bar{S}_{kk}^M(\omega)}} \quad (3)$$

The diagrams of lagged coherency in the frequency range 0-10Hz, where the frequencies of all significant modes of a structure are expected to be, computed individually for the longitudinal, transverse and vertical component of the recorded motions are illustrated in Figure 4 for pairs M4-M5, M4-M6 and M4-M7, in Figure 5 for pairs M5-M6 and M5-M7 and in Figure 6 for pair M6-M7. As anticipated, the coherency loss increases with increasing separation distance and frequency.
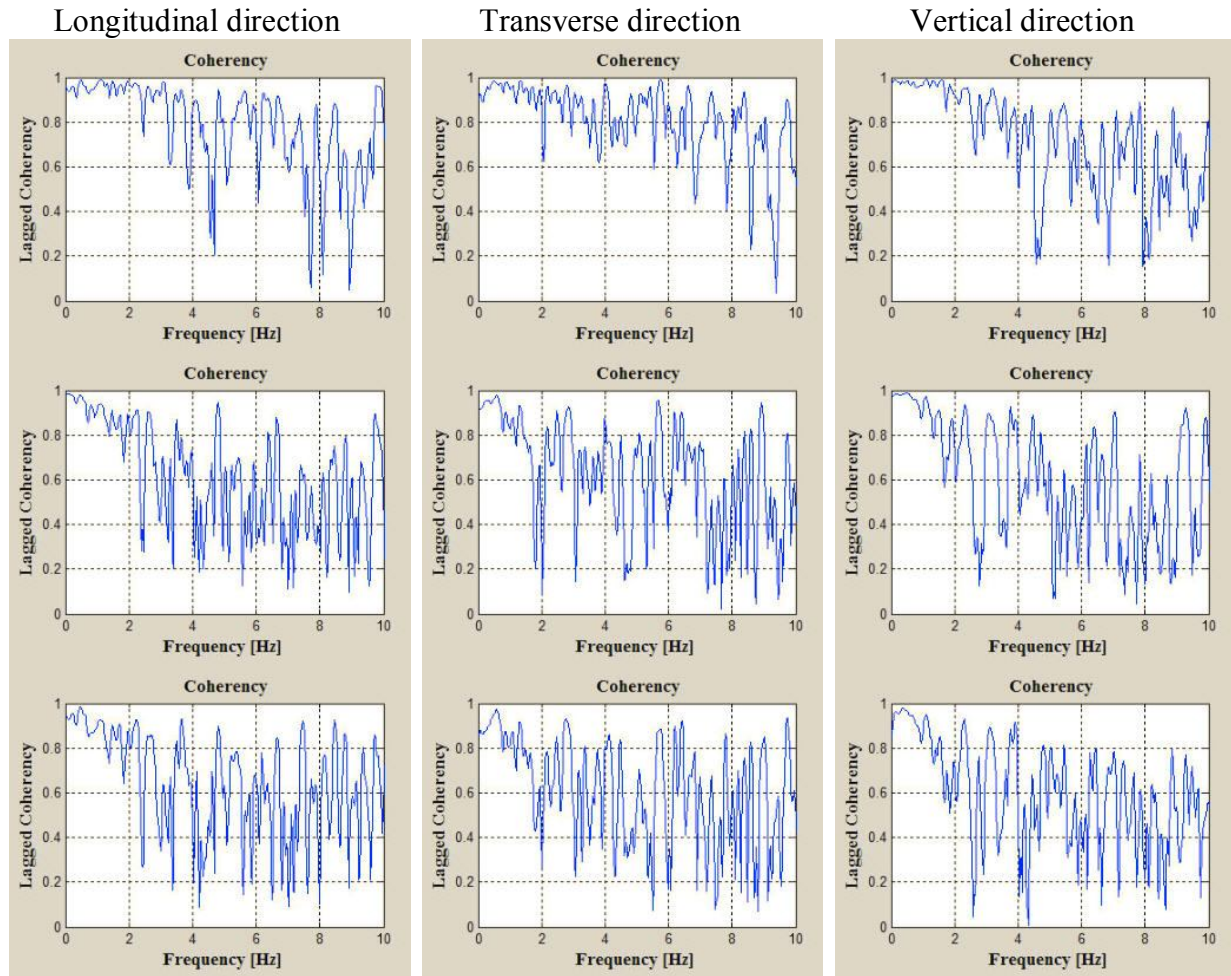

Figure 4: Lagged coherency of motions recorded between piers M4-M5 (at distance l=90m, top), M4-M6 (at distance l=305m, middle) and M4-M7 (at distance l=395m, bottom).

Longitudinal direction   Transverse direction   Vertical direction
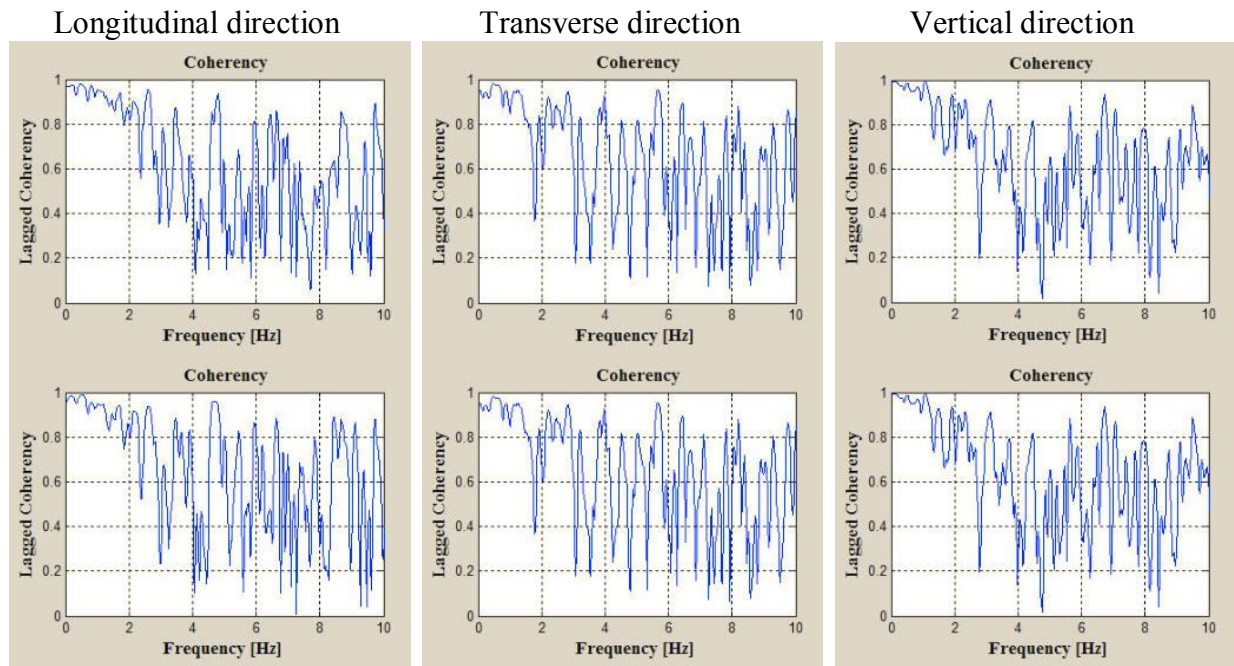

Figure 5: Lagged coherency of motions recorded between piers M5-M6 (at distance l=215m, top), and M5-M7 (at distance l=305m, bottom).

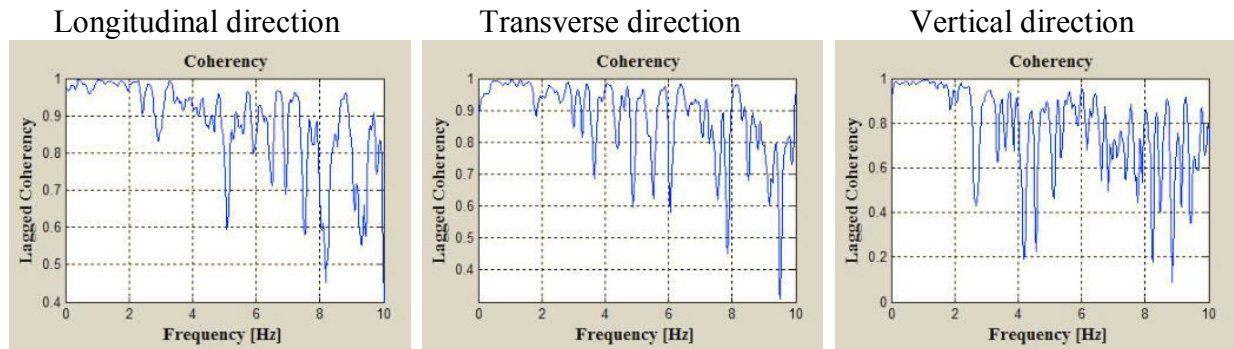Longitudinal direction   Transverse direction   Vertical direction

Figure 6: Lagged coherency of the motions recorded between piers M6-M7 (at distance l=90m).

The comparison of the computed incoherencies with one of the most commonly used patterns proposed by Luco and Wong [12] is made in Figure 7, where the lagged coherency is given by the following expression:

$$|\gamma(\xi,\omega)| = e^{-\left(\frac{v\omega\xi}{V_s}\right)^2} = e^{-a^2\omega^2\xi^2} \tag{4}$$

In eq. (4), the coherency drop parameter α controls the exponential decay and ξ is the distance between the two stations examined. Typically, α is taken equal to 2.5×10^{-4}sec/m; however, comparison for the case of motions recorded along the longitudinal direction at the bases of the piers M4 and M7 (i.e., at separation distance ξ=395m) reveals that a value of α equal to 0.5×10^{-4}sec/m leads to better matching with the observed incoherency.
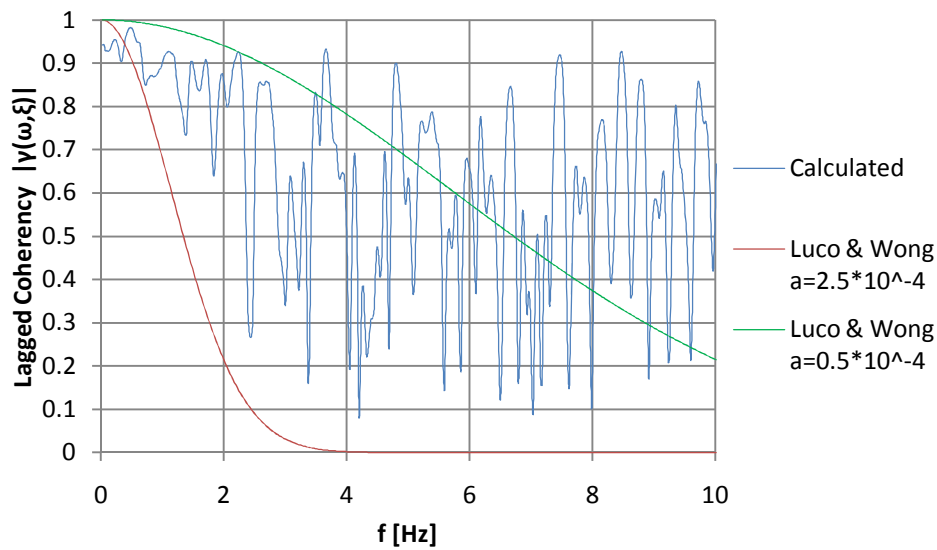
Figure 7: Comparison between observed and predicted coherency loss for different values of the Luco and Wong model [12].

4 ANALYSES PERFORMED

Most analytical or numerical studies investigating the effects of spatial variability of earthquake ground motion on the response of bridges compare the results of multiple-support excitation analysis with those of a reference condition which typically assumes synchronous excitation among all bridge supports. The comparison can then be made in terms of a ratio of the action effects (forces or displacements) of specific structural components over the response under synchronous conditions.

In the case examined herein though, the fact that the ground motions have been recorded at the bases of the four bridge piers leads to a realistic excitation scenario with respect to the actual seismo-tectonic and soil conditions of the site under study but at the same time makes it difficult to assume the corresponding compatible "synchronous" excitation conditions. One option would have been to pick one of the recorded motions and apply it synchronously at all pier supports; however, this option is limited by the fact that the available records show significant discrepancy in terms of both their PGA and spectral amplification, primarily due to local site effects at the location of pier M5 (Figure 8).

In order to overcome this difficulty, it was decided to adopt the following procedure: as the strongest component of the motions recorded is in the longitudinal direction, all records (in all components) are scaled (Table 1) to the average spectral acceleration of all records at period T=1.64sec, which is the period of the highest contributing mode, activating 76% of the mass in the longitudinal direction (Table 2). Then, four different "synchronous" excitation scenarios are developed, assuming each time that the scaled motions in piers M4, M5, M6 and M7 respectively, are applied uniformly at all supports. Given the aforementioned scaling, it is deemed that the four different versions of uniform excitation are compatible in terms of spectral amplification (at least at the period of vibration that is affected by the dominant earthquake component), while the fact that all the resulting scaling factors are close to unity, guarantees that the scaling-induced dispersion is limited.

Based on the above, five non-linear dynamic analyses of the Evripos cable-stayed bridge are performed using the computer program SAP2000 [13], that is one using the recorded set of motions and four considering the aforementioned compatible "synchronous" excitation

scenarios. All three components of the motions were applied simultaneously. The geometrical non-linearity induced by the bridge cables was considered assuming tension-only capabilities and the initial cable stress state due to dead loading was applied through non-linear staged-construction static analysis.

Beam elements were used to model the piers, while the bridge deck was simulated by shell elements. Piers were assumed fixed at their bases while the supporting conditions at the two bridge edges were considered as rolled in the longitudinal direction and pined in the transverse.
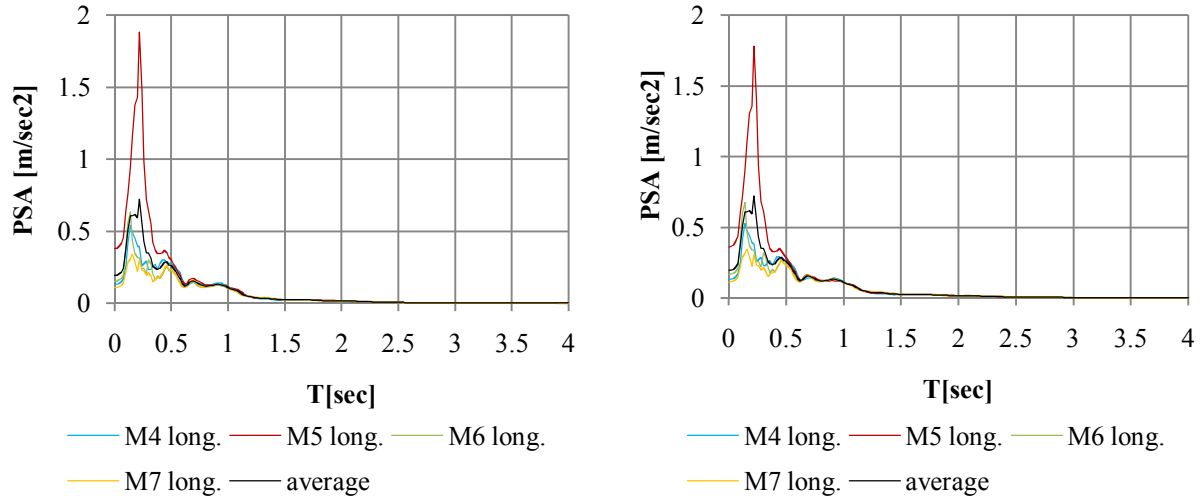

Figure 8: 5% damped elastic response spectra of the longitudinal components of the records at piers M4, M5, M6, M7 compared to the average response spectrum.

Pier	M4	M5	M6	M7
Scale factor	0.977	0.947	1.069	1.014

Table 1: The scaling factors for the records at M4, M5, M6 and M7 so as to their response spectra to have the PSA with the average response spectrum for T=1.64sec.

Mode ID	Period	UX	UY	UZ	RX	RY	RZ
#1	2.712	0	0	6.7	1.2	2.3	0
#2	2.385	20.2	0	0	0	0	0
#3	2.061	0	58.3	0	3.4	0	47.2
#4	1.645	76.3	0	0	0	0	0
#5	1.298	0	0	6.2	1.4	5.5	0
#9	1.065	0	0	37.4	7.3	28.8	0

Table 2: Dynamic characteristics (eigenfrequencies and corresponding modal contribution) of the Evripos cable-stayed bridge.

The amplitude of the seismic moments (i.e., the earthquake-induced bending moments at the bases of piers M4 and M7 and at one of the two columns at each pier M5 and M6), the displacements at the top of each pier and the displacements in the middle of the deck are examined for all asynchronous and synchronous excitation cases previously presented.

Figure 9 presents the comparison between the computed seismic moments at the base of pier M6 using the Athens 1999 (asynchronous) recorded motions, and those computed through the four "synchronous" excitation scenarios, that is, by the uniform application of records M4, M5, M6, and M7 respectively. The comparison of the maxima among all cases are summarized in Table 3. It can be seen that the moments M_2 developed at the base of pier M6 transversely to the bridge plane, due to the asynchronous recorded ground motions is systematically lower regardless of the "synchronous" excitation pattern adopted. As anticipated, this is more intense (approximately 32%) for the synchronous case involving the uniform application of record M5, which, despite of the scaling to a common level of spectral amplification, still corresponds to the highest PGA among the records at all locations. On the other hand, the situation reverses for the bending moments M_3 within the bridge plane and the asynchronous excitation results in higher levels of stress in all cases, reaching 43% increase in the extreme case of applying record M7 uniformly at all support points. The respective results for pier M5 are also summarized in Table 3. It can be seen that seismically-induced bending moments in both directions are decreased when assuming uniform excitation conditions independently of the scenario adopted.

As far as the displacements are concerned, the corresponding time histories are plotted in Figures 10, 11 and 12 for the middle of the central span and the top of the pylons M5 and M6 respectively, while the maximum in time displacements are compared in Tables 4, 5 and 6. More specifically, asynchronous excitation is systematically favorable for the span middle deck displacements which are decreased up to 36%, 45% and 63% along the three principal direction U_x, U_y and U_z. The same trend is also observed for the case of the top of the M5 pylon - though to a lesser degree - and with the exception of a minor (6%) increase in vertical displacements for one of the scenarios studied. In contrast to the above, the displacements at the top of pylon M6 derived under the asynchronous recorded ground motions are generally increased compared to the synchronous case and are almost double (increased by 82%) when compared to the uniform application of record M4. Vertical displacements are also increased up to 11% due to asynchronous motion.

Uniform excitation scenario	Case studied	Pier M5		Pier M6	
		M_2 [kNm]	M_3[kNm]	M_2[kNm]	M_3[kNm]
Synch M4	Synch	1350.70	798.54	1338.30	759.11
	Asynch	833.53	743.05	949.48	943.70
	Asyn/Sync-1	*-38%*	*-7%*	*-29%*	*+24%*
Synch M5	Synch	1510.39	1008.53	1403.31	919.10
	Asynch	833.53	743.05	949.48	943.70
	Asyn/Sync-1	*-45%*	*-26%*	*-32%*	*+3%*
Synch M6	Synch	1401.33	981.36	1345.28	815.00
	Asynch	833.53	743.05	949.48	943.70
	Asyn/Sync-1	*-41%*	*-24%*	*-29%*	*+16%*
Synch M7	Synch	1314.79	849.06	1335.77	658.05
	Asynch	833.53	743.05	949.48	943.70
	Asyn/Sync-1	*-37%*	*-13%*	*-29%*	*+43%*

Table 3: Comparison of maximum absolute earthquake-induced bending moments developed in pier M6 for synchronous and asynchronous excitation (cases M4, M5, M6, M7).
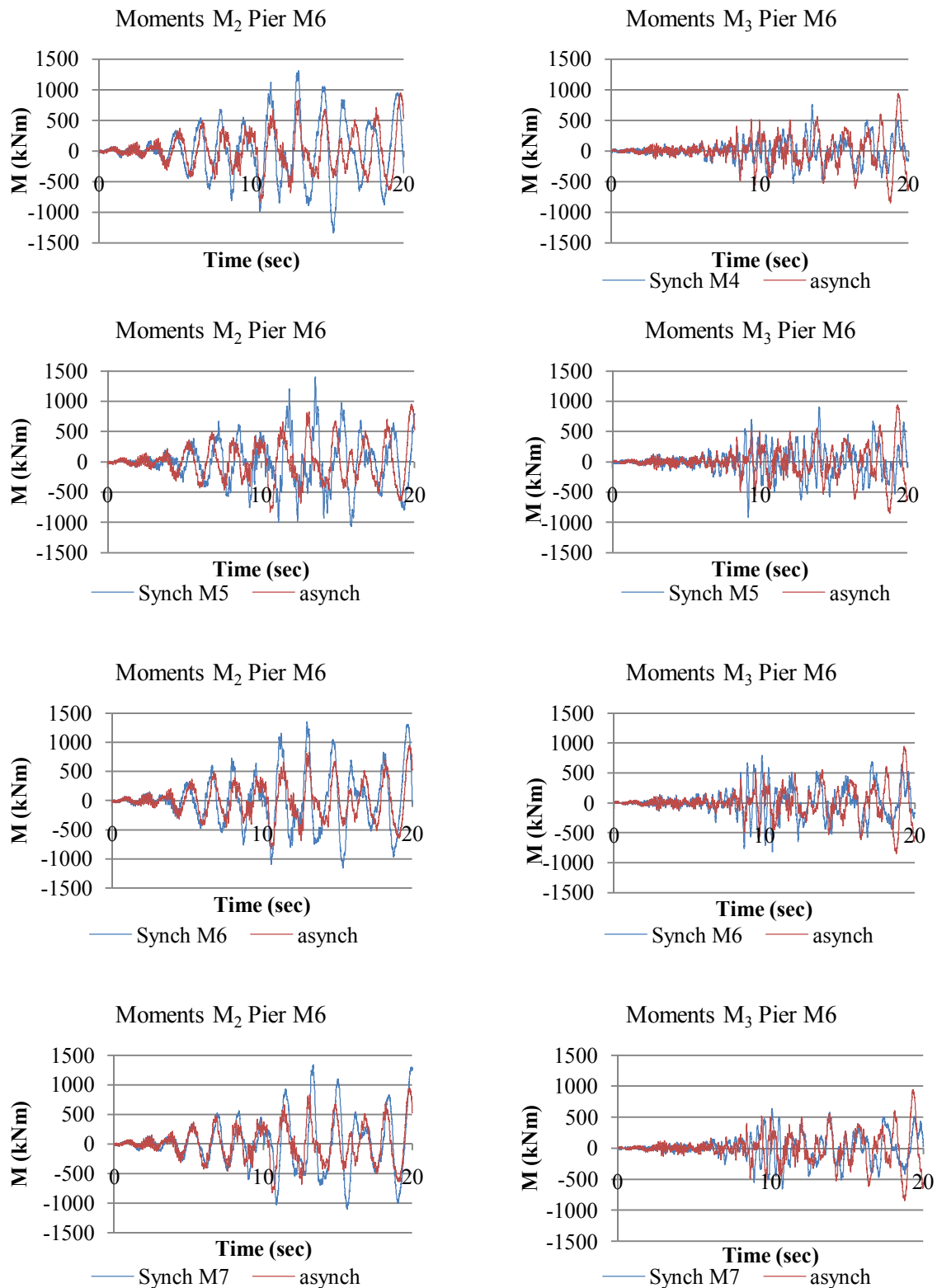
Figure 9: Comparison of the computed seismic moments at the base of pier M6 using the Athens 1999 (asynchronous) recorded motions, with those computed through the four "synchronous" excitation scenarios (uniform application of records M4, M5, M6, M7 respectively).
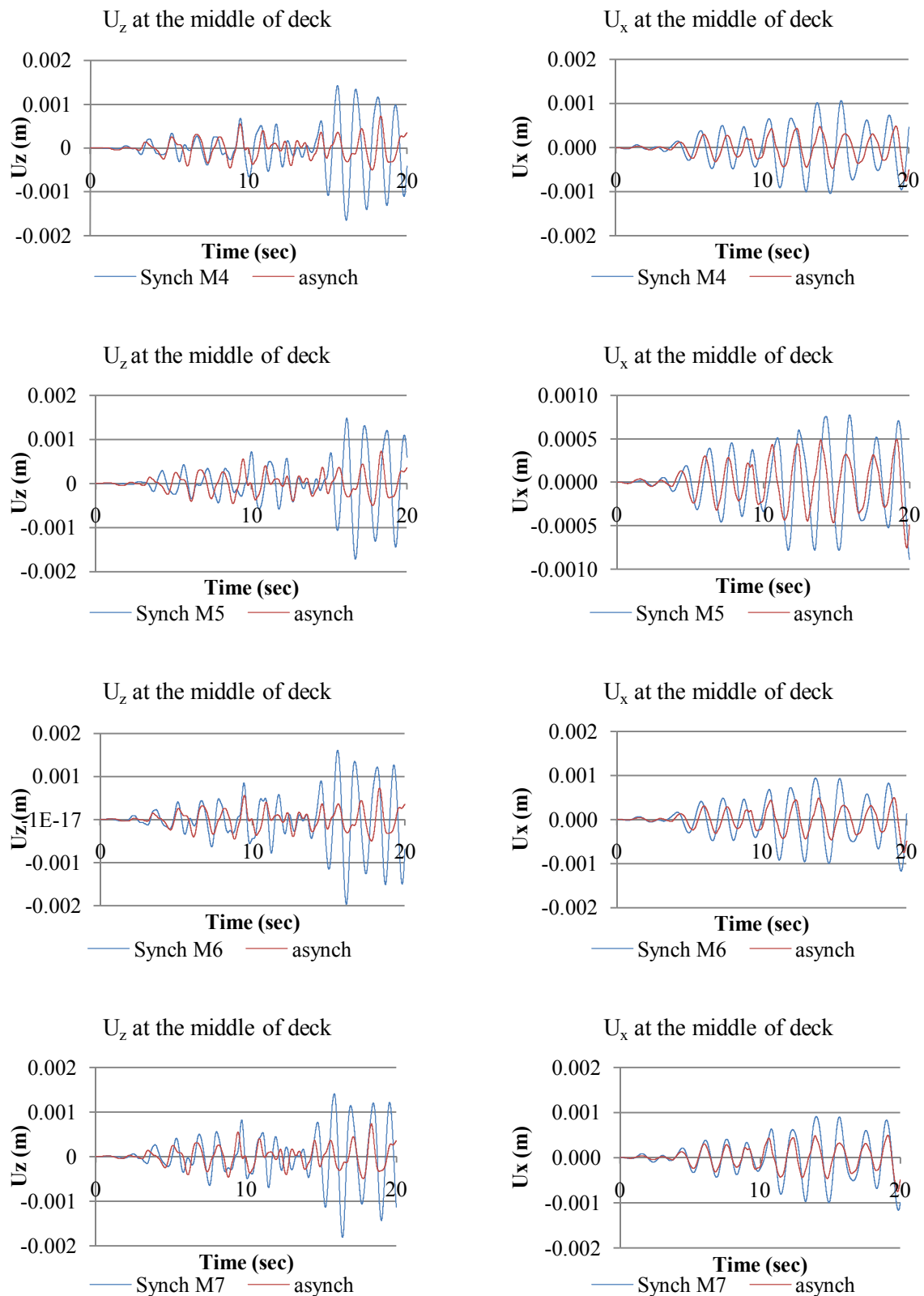
Figure 10: Comparison of the seismic deck displacements in the middle of the central span using the Athens 1999 (asynchronous) recorded motions, with those computed through the four "synchronous" excitation scenarios (uniform application of records M4, M5, M6, M7 respectively).

Displacements at the middle of the bridge deck (cm)				
Uniform excitation scenario	Case studied	U_x	U_y	U_z
Synch M4	Synch	0.11	0.14	0.16
	Asynch	0.08	0.10	0.07
	Asyn/Syn-1	*-28%*	*-25%*	*-56%*
Synch M5	Synch	0.09	0.14	0.17
	Asynch	0.08	0.10	0.07
	Asyn/Syn-1	*-15%*	*-29%*	*-58%*
Synch M6	Synch	0.12	0.18	0.20
	Asynch	0.08	0.10	0.07
	Asyn/Syn-1	*-36%*	*-45%*	*-63%*
Synch M7	Synch	0.12	0.16	0.18
	Asynch	0.08	0.10	0.07
	Asyn/Syn-1	*-36%*	*-41%*	*-60%*

Table 4: Maximum values of absolute displacements [cm] which developed due to asynchronous and synchronous (M4, M5, M6, M7) excitation scenarios at the middle of the bridge deck.

Displacements at the pier M5 top [cm]				
Uniform excitation scenario	Case studied	U_x	U_y	U_z
Synch M4	Synch	0.09	0.18	0.05
	Asynch	0.07	0.16	0.05
	Asyn/Syn-1	*-22%*	*-12%*	*+7%*
Synch M5	Synch	0.067	0.23	0.05
	Asynch	0.071	0.16	0.05
	Asyn/Syn-1	*+6%*	*-34%*	*0%*
Synch M6	Synch	0.09	0.27	0.06
	Asynch	0.07	0.16	0.05
	Asyn/Syn-1	*-20%*	*-42%*	*-14%*
Synch M7	Synch	0.09	0.25	0.05
	Asynch	0.07	0.16	0.05
	Asyn/Syn-1	*-23%*	*-37%*	*-6%*

Table 5: Maximum values of absolute displacements [cm] which developed due to asynchronous and synchronous (M4, M5, M6, M7) excitation scenarios at the top of pier M5.
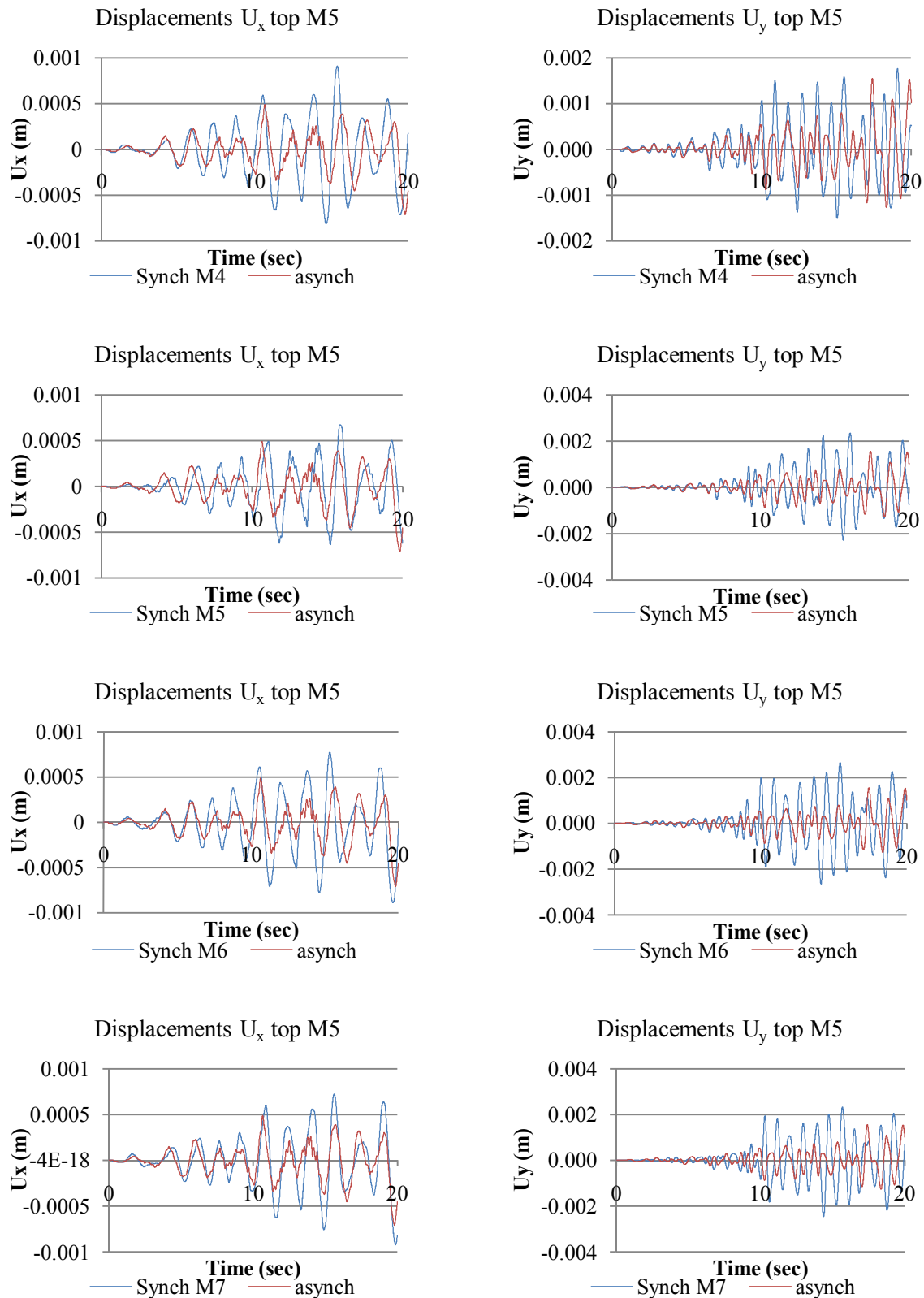
Figure 11: Comparison of the seismic displacements at the top of the pylon at the location of pier M5 using the Athens 1999 (asynchronous) recorded motions, with those computed through the four "synchronous" excitation scenarios (uniform application of records M4, M5, M6, M7 respectively).
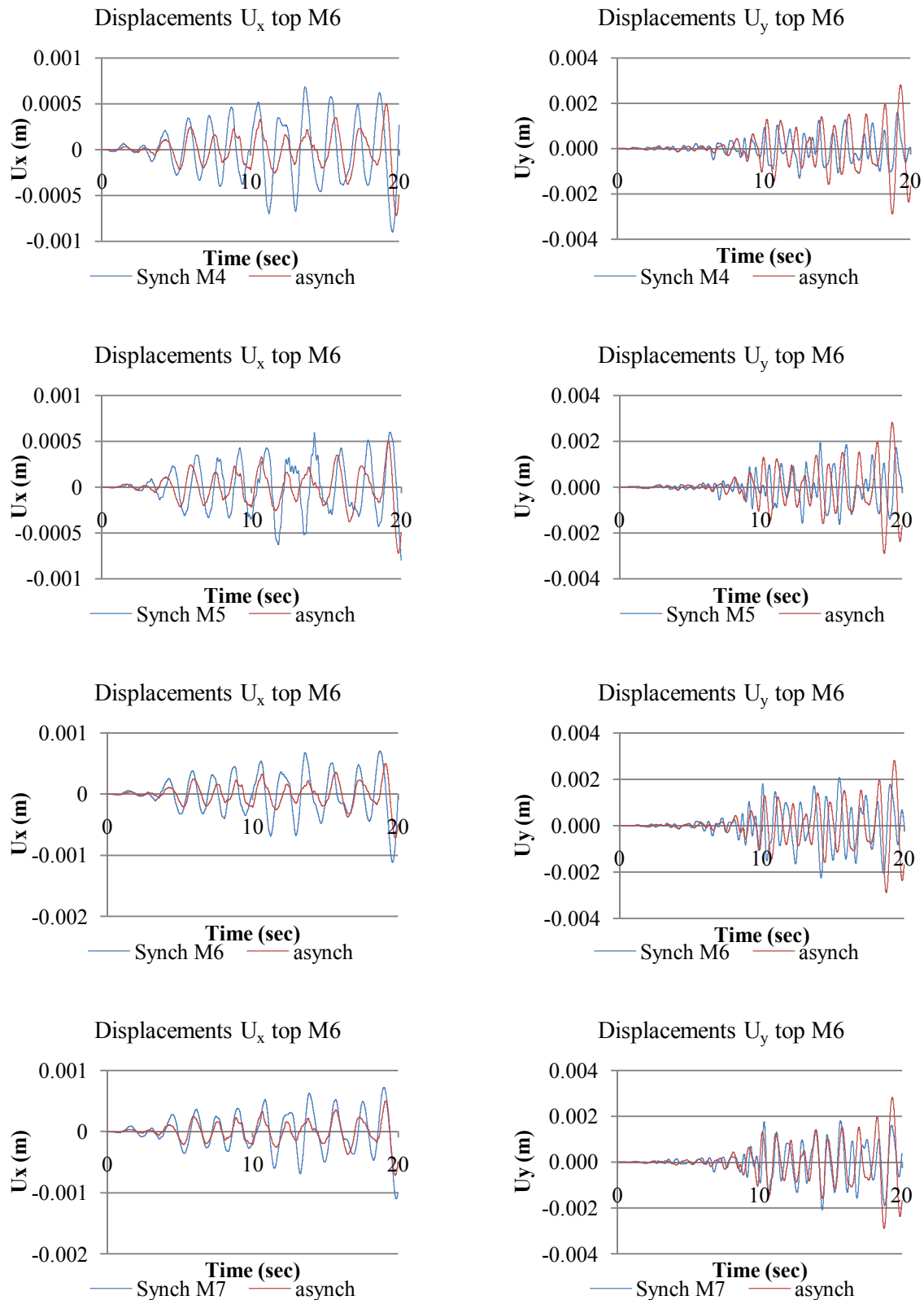
Figure 12: Comparison of the seismic displacements at the top of the pylon at the location of pier M6 using the Athens 1999 (asynchronous) recorded motions, with those computed through the four "synchronous" excitation scenarios (uniform application of records M4, M5, M6, M7 respectively).

Displacements at the pier M6 top [cm]				
Uniform excitation scenario	Case studied	U_x	U_y	U_z
Synch M4	Synch	0.09	0.16	0.04
	Asynch	0.07	0.29	0.05
	Asyn/Syn-1	*-20%*	*+82%*	*+11%*
Synch M5	Synch	0.08	0.19	0.047
	Asynch	0.07	0.29	0.049
	Asyn/Syn-1	*-10%*	*+49%*	*+4%*
Synch M6	Synch	0.11	0.23	0.054
	Asynch	0.07	0.29	0.049
	Asyn/Syn-1	*-36%*	*+28%*	*-9%*
Synch M7	Synch	0.11	0.21	0.050
	Asynch	0.07	0.29	0.049
	Asyn/Syn-1	*-35%*	*+38%*	*-2%*

Table 6: Maximum absolute values of displacements [cm] which developed due to asynchronous and synchronous (M4, M5, M6, M7) excitation at the pier M6 top. In last row is presented the rate of increase or decrease.

These results indicate that the complex inherent nature of ground motion incoherency are strongly correlated to the dynamic characteristics of the excited structure and do not systematically lead to uniform increase or decrease of the corresponding action effects. For this reason, it was deemed useful to investigate further the significance of the potential excitation of higher structural modes for which there are strong indications ([2], [7], [14]) that it is one of the key features of multiple support excitation.

It has to be noted that due to the cable suspension of the Evripos bridge, the associated geometrical non-linearities make it difficult to spot specific, load independent, modes of vibration. However, it was computationally verified that the low level of excitation of the event considered in this work (which does not exceed 0.032g) does not lead to any untensioning of the suspension cables, thus ensuring that at least for the particular earthquake intensity, the eigen-frequencies summarized in Table 2 still hold.

In order to examine the higher modes excitation, the Fourier spectra of the accelerations were plotted at the same points as for the displacements (Figures 13 and 14). As the analysis is in fact linear elastic, (since the dynamic characteristics remain constant during the studied excitation), the frequencies where the peaks of the Fourier spectra are observed coincide with the eigen-frequencies of the structure. In principle, one would expect that the decreased response due to asynchronous excitation observed in Figures 9-12 should correlate well with the decrease of the Fourier amplitudes at the corresponding frequencies of the associated modes.

Indeed, Figure 13 shows a clear reduction in the Fourier amplitudes of acceleration at the middle of the central span, at the period of 1.64 sec, which corresponds to the 4th mode activating 76% of mass in the longitudinal direction when the response under the recorded asynchronous excitation is compared to that of the uniform application of the M5 record. This is in good agreement with the decrease in both bending moments and displacements summarized in Table 4. The same correlation is observed with respect to the vertical direction where the Fourier amplitudes are decreased at periods 1.30 sec and 1.06 sec corresponding to the 5th

mode (activating 6.5% of mass in the vertical direction) and 9th mode (activating 37% of mass in the vertical direction) respectively; a fact that is also in line with the favorable effect of asynchronous excitation in Table 4.
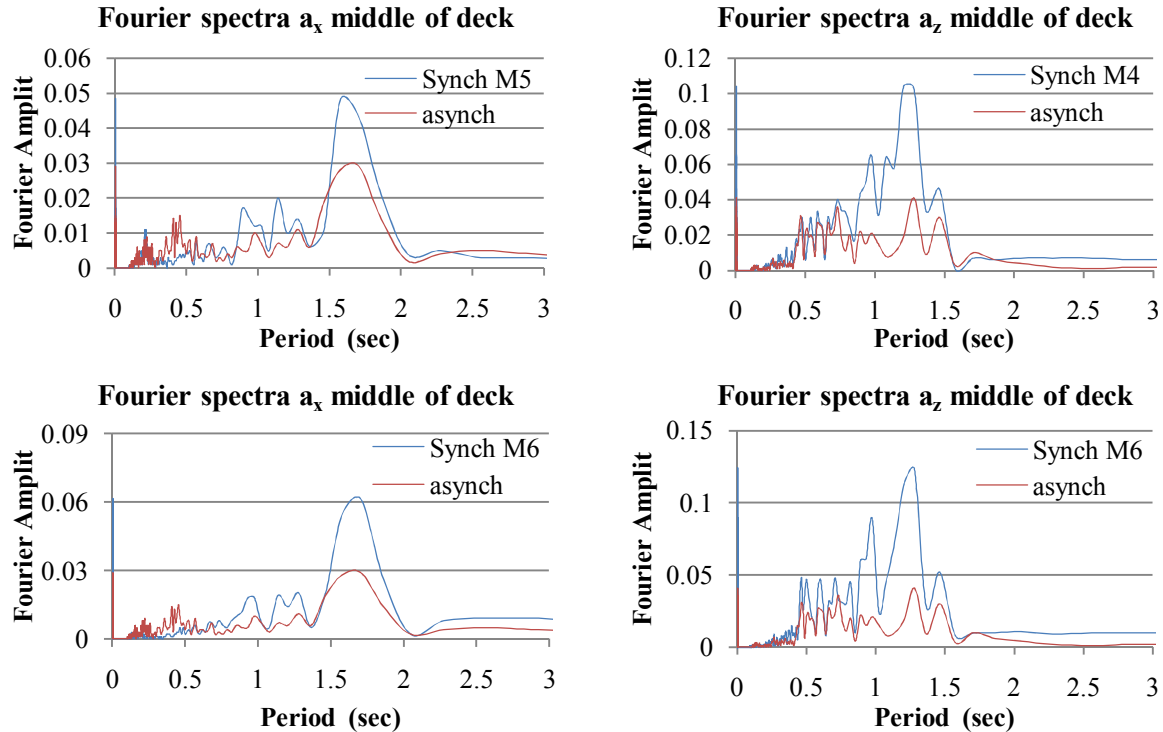

Figure 13: Comparison of the Fourier spectra of the accelerations computed in the longitudinal and vertical direction at the middle of the deck using the Athens 1999 (asynchronous) recorded motions, with those computed by the four "synchronous" excitation scenarios (uniform application of records M4, M5, M6, M7 respectively).

Similarly to the above, when the comparison is made on the basis of the uniform application of record M5, the reduction of the Fourier amplitudes at periods 2.38 sec (2nd mode-activating 20% in the longitudinal direction) and 1.64 sec (4th mode-activating 76% in the longitudinal direction) is confirmed with the response reduction in Table 4. Again, good correlation is observed for the vertical direction, where the reduction of the Fourier amplitudes takes place at periods 1.3 sec (5th mode-activating 6.5% in the vertical direction), 1.06 sec (9th mode-activating 37% in the vertical direction) and 0.82 sec (15th mode-activating 68% in the same direction) and the comparison of the maxima in the time domain depicted in Table 4. It is noted that the same trend is also observed in numerous locations of the bridge.
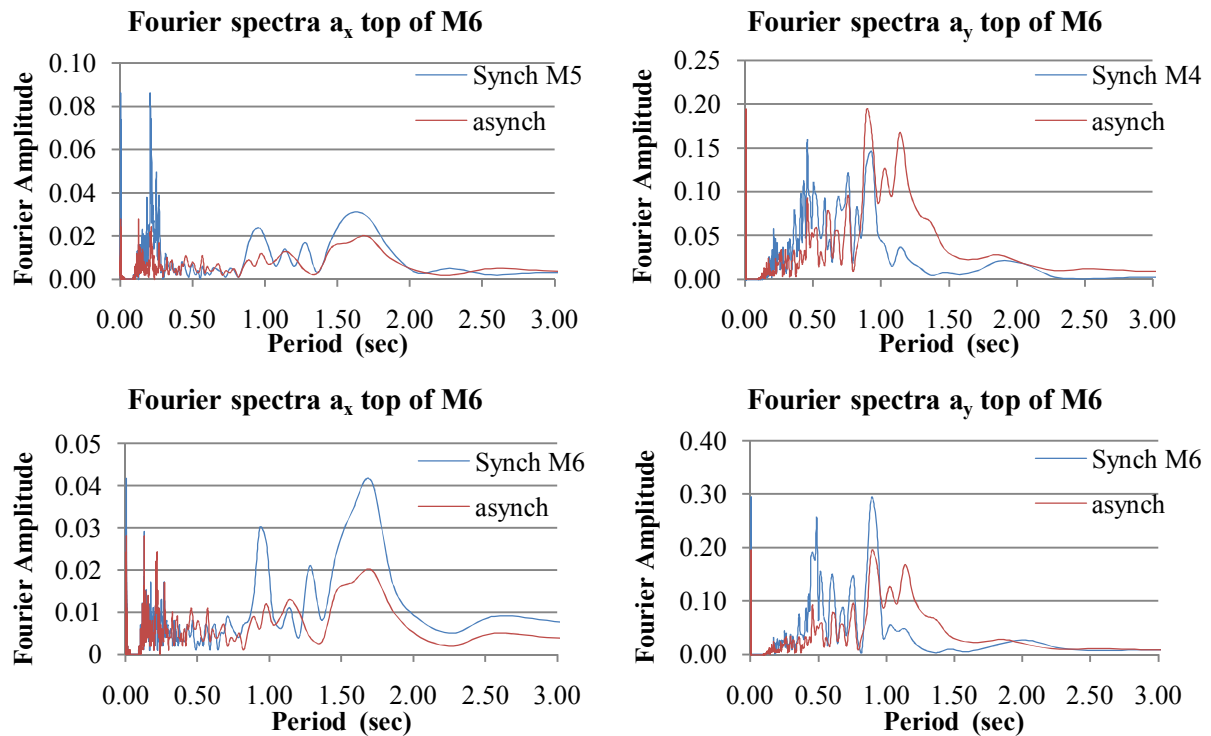
Figure 14: Comparison of the Fourier spectra of the accelerations computed in the longitudinal and vertical direction at the top of the pylon of M6 using the Athens 1999 (asynchronous) recorded motions, with those computed by the four "synchronous" excitation scenarios (uniform application of records M4, M5, M6, M7).
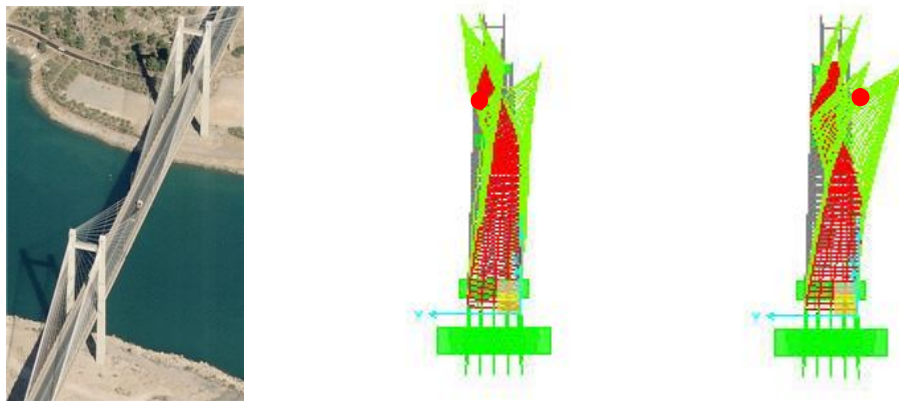

Figure 15: Characteristic antisymmetric (mode 8: T=1.11sec, R_z=10%, middle) and symmetric (mode 11: T=0.89, U_y=10.7%, left) mode shapes, excited due to asynchronous excitation.

Figure 14 presents the Fourier spectra of the accelerations in the longitudinal and transverse directions at the top of the M6 pylon. When the comparison is made on the basis of the uniform application of the M5 record, a reduction of the Fourier amplitudes is first observed at periods 2.38 sec (corresponding to the 2nd mode, activating 20% of the mass in the longitudinal direction) and 1.64 sec (4th mode, activating 76% of the mass in the same direction), which justifies the reduction of the displacements documented in Table 6. On the other hand, when the transverse direction is examined, a remarkable amplification is observed at period 0.89 sec corresponding to the symmetric 11th mode, activating 10.7% of the mass in the trans-

verse direction, while significant amplification is also depicted at period T=1.11 sec which corresponds to the antisymmetric 8th mode (activating 9.8% of the mass around the z axis). Both mode shares are illustrated in Figure 15 where it is clearly seen that the transverse displacement of the top of the M6 pylon is very much affected by the excitation of the particular modes. As a result, the good correlation between the excited higher modes of vibration due to asynchronous earthquake motion and the corresponding impact of the latter on the overall bridge response is also confirmed for the case of the particular cable-stayed bridge. This observation is deemed interesting, especially bearing in mind that it has been made for the case of a real bridge using recorded earthquake ground motions.

5 CONCLUSIONS

The scope of this study was to examine the effects of asynchronous excitation on the Evripos cable-stayed bridge, utilizing the recorded response at four locations of the accelerometer network maintained by ITSAK, due to the M_s=5.9, 7/9/1999 Athens earthquake. The records were filtered to remove inertial interaction effects and their coherency was computed for all available record pairs. A detailed finite element model of the cable-stayed bridge was developed and its response was computed using both the recorded motions and four synchronous excitation scenarios. The comparative study of the results indicates that:

- For the particular bridge studied, spatial variability of seismic ground motion has a generally favorable effect, at least on the pier base bending moments and the displacements middle of the central span deck. Apparently, the extent of this beneficial phenomenon is very much dependent on the assumptions made regarding the definition of the "synchronous" excitation, which, in contrast to the actual, recorded asynchronous case, is not obvious.

- There are specific cases (i.e., out-of-plane bending moments and displacements at the top of the two bridge pylons) where the asynchronous excitation has a clearly critical effect.

- In all cases, the observed deamplification or amplification of the bridge displacements was verified by the reduced or increased amplitude of the Fourier spectra respectively, at selected frequencies, which correspond to specific modes that have a strong impact on the vibration of the structure along the directions examined. It is believed that, given the complexity of the problem studied, the potential excitation of higher modes due to asynchronous excitation may be a key tool for understanding the role of spatial variability of earthquake ground motion on the overall seismic response of bridges.

REFERENCES

[1]   G. Deodatis, V. Saxena, and M. Shinozuka, "Effect of spatial variability of ground motion on bridge fragility curves," *8th ASCE Specialty Conference on Probabilistic Mechanics and Structural Reliability*, 2000, pp. 1-6.

[2]   A.G. Sextos, A.J. Kappos, and K.D. Pitilakis, "Inelastic dynamic analysis of RC bridges accounting for spatial variability of ground motion, site effects and soil-

structure interaction phenomena. Part 2: Parametric study," *Earthquake Engineering & Structural Dynamics*, vol. 32, 2003, pp. 629-652.

[3]   A. Lupoi, P. Franchin, P.E. Pinto, and G. Monti, "Seismic design of bridges accounting for spatial variability of ground motion," *Earthquake Engineering and Structural Dynamics*, vol. 34, 2005, pp. 327-348.

[4]   N.J. Burdette and A.S. Elnashai, "Effect of Asynchronous Earthquake Motion on Complex Bridges. II: Results and Implications on Assessment," *Journal of Bridge Engineering*, vol. 13(2), 2008, pp. 166-172.

[5]   A.S. Nazmy and A.M. Abdeel-Ghaffar, "Effect of ground motion spatial variability on the response of cable-stayed bridges", Earthquake Engineering and Structural Dynamics, vol. 21, 1992, pp.1-20.

[6]   N.A.Abrahamson, "Spatial variation of multiple support inputs," Proceedings of the 1st U.S. Seminar on Seismic Evaluation and Retrofit of Steel Bridges. A Caltrans and University of California at Berkeley Seminar, San Francisco, CA, 1993.

[7]   A.G. Sextos and A.J. Kappos, "Evaluation of seismic response of bridges under asynchronous excitation and comparisons with Eurocode 8-2 provisions", *Bulletin of Earthquake Engineering*, vol. 7, 2009, pp. 519-545.

[8]   V. Lekidis, M. Tsakiri, K. Makra, C. Karakostas, N. Klimis, and I. Sous, "Evaluation of dynamic response and local soil effects of the Evripos cable-stayed bridge using multi-sensor monitoring systems", *Engineering Geology*, vol. 79, 2005, pp. 43-59.

[9]   V. Lekidis, "Investigation of the seismic response of the Evripos high bridge: Experimental and analytical approach", Technical Report, Institute of Engineering Seismology and Earthquake Engineering, Thessaloniki: 2003 (in Greek).

[10] N.A. Abrahamson, J.F. Schneider, and J.C. Stepp, "Empirical spatial coherency functions for applications to soil-structure interaction analyses", *Earthquake Spectra*, vol. 7, 1991, pp. 1-28.

[11] A. Zerva, *Spatial Variation of Seismic Ground Motions-Modelling and Engineering Applications*, CRC Press, Taylor & Francis Group, FL, 2009.

[12] J.E.Luco and H.L.Wong, "Response of a rigid foundation to a spatially random ground motion," Earthquake Engineering and Structural Dynamics, Vol. 14, 1986, pp.891-908.

[13] CSI, *SAP 2000* Nonlinear Ver. 10.01, *User's Reference Manual*, *Berkeley*, California, U.S.

[14] T.E. Price and M.O. Eberhard, "Effects of Spatially Varying Ground Motions on Short Bridges", *Journal of Structural Engineering*, vol. 124(8), 1998, pp. 948-955.